ResearchGate

See discussions, stats, and author profiles for this publication at: https://www.researchgate.net/publication/231632785

High Overtones of the C−H Stretching Vibrations in Anisole and Thioanisole

ARTICLE *in* THE JOURNAL OF PHYSICAL CHEMISTRY A · NOVEMBER 2002

Impact Factor: 2.69 · DOI: 10.1021/jp020691g

CITATIONS
15

READS
44

3 AUTHORS, INCLUDING:

Maurizio Muniz-Miranda
University of Florence
202 PUBLICATIONS **2,082** CITATIONS

SEE PROFILE

Available from: Maurizio Muniz-Miranda
Retrieved on: 23 January 2016

High Overtones of the C−H Stretching Vibrations in Anisole and Thioanisole

Cristina Gellini, Laura Moroni, and Maurizio Muniz-Miranda*

Dipartimento di Chimica, Universita' di Firenze, Via della Lastruccia 3, I-50019 Sesto Fiorentino, Firenze, Italy

Received: March 12, 2002; In Final Form: June 18, 2002

The high overtone C−H stretching vibrations of anisole and thioanisole have been measured in liquid phases by using optical absorption and optoacoustic spectroscopy. The local mode model satisfactorily describes the experimental data and provides anharmonicities and force constants. The data obtained by the DFT calculations allow a complete assignment of all the observed bands in the vibrational spectra of the two molecules. The comparative analysis of the overtone spectra and of the DFT results confirms the occurrence of the methyl C−H symmetric stretching at low wavenumber (∼2836 cm^{-1}) in anisole as due to a strong anharmonic coupling, deriving from a Fermi resonance with the first overtone of the methyl symmetric deformation mode. This effect is typical of the methoxy group, because it does not occur in thioanisole as well as in toluene. The present investigation demonstrates the existence of a strong effect of electron conjugation of OCH_3 toward the aromatic system, in comparison with the SCH_3 group, as evidenced also by the study of the rotational barriers and the proton magnetic resonance data.

Introduction

The experimental investigation on highly excited vibrational levels in the electronic ground state of a molecule can offer useful information on different processes, such as photodissociations, radiationless transitions, and chemical reactions for the bonds involved in the vibrations. Actually, the properties of the high overtone spectra of C−H stretching modes are mainly due to the local environment of the bonds, thus conformational[1,2] and steric[3] different situations can be analyzed. In addition, the experimental data obtained from these spectra can be correlated with the substituent effect and the inductive contribution, as performed in the case of monosubstituted benzenes.[4] By this technique, bond lengths and force constants were usually estimated and compared with the corresponding values found by microwave spectra and vibrational analysis, respectively.[5−8] Finally, a relation with chemical shifts in proton magnetic resonance was found in cyclic compounds, where aromaticity was responsible for a significant electron current in the ring.[8,9]

The C−H stretching overtone spectra are characterized by one peak for each of the nonequivalent C−H oscillators in a molecule and can be interpreted within the local mode model of molecular vibrations.[10−14] In this model, the C−H bond vibrations behave as highly anharmonic localized modes, with harmonic interbond coupling. In the ordinary normal mode approach, instead, the stretching vibrations are represented as harmonic oscillators, perturbed and coupled by anharmonic Darling-Dennison interactions.[15] Actually, the two pictures correspond to a different choise of basis functions and should give theoretically identical results,[16] if all the calculations were done without any approximations. If, instead, only the simplest contents of the local mode theory are adopted, as in the case proposed for dihalomethanes,[17] this equivalence is obviously no longer valid. At low energies, as in the case of low values of the vibrational quantum number, the coupling between these nearly resonant oscillators is effective and the normal mode description is a valid approximation. At higher energies, as in the case of high overtones, the bonds are detuned from resonance and the local mode model, in terms of isolated oscillators, is more appropriate. The validity of this latter approach closely depends on the quenching of the interbond coupling by the effect of the bond anharmonicity at high energies. Thus, delocalized modes, involving two or more vibrating bonds, still occur in high overtones, while the stretching motions of single bonds, like C−H stretching vibrations, are more anharmonic and can be correctly represented as uncoupled oscillators.

Thermal lensing[10,18] and optoacoustic spectroscopy[19,20] are the most common techniques for investigating high overtone spectra as valid alternatives to the optical absorption spectroscopy, mainly for liquid-phase samples. In a liquid environment, however, the lines are generally too broad for the resolution of the bands corresponding to nonequivalent C−H stretching vibrations of the same kind. Much narrower lines, instead, are detected by overtone spectra in the gas phase, where several studies were performed.[2,21−24] On the other hand, intermolecular interactions in the liquid phase can be suitably analyzed in the overtone spectra, as recently performed in the case of isoxazole and thiazole.[9] In the present work, optical absorption spectroscopy and optoacoustic spectroscopy have been employed for the study of liquid anisole and thioanisole (Figure 1), up to the sixth overtones of the C−H stretching vibrations of aryl and methyl groups. Moreover, density functional theory (DFT) calculations are here combined with the study of the high overtones, in terms of local mode model. The aim is to study the effect of the different heteroatoms on the methyl and aryl CH stretching modes, in relation with the structural arrangements of the molecules. Actually, oxygen and sulfur have different electronegativities, even if both OCH_3 and SCH_3 groups may give rise to π-electron conjugation with the aromatic system. In addition, these groups exhibit some rotational freedom, which can induce changes in static and dynamic properties of the molecules and that have been investigated in the present work. Detailed experimental data on their molecular structures are not present in the literature, except partial information on the

* Corresponding author. E-mail: muniz@chim.unifi.it.

10.1021/jp020691g CCC: $22.00 © 2002 American Chemical Society
Published on Web 10/26/2002

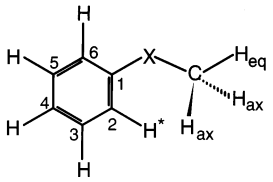

Figure 1. Molecular structure of anisole and thioanisole; "eq" = equatorial, "ax" = axial.

substituent groups, as obtained by microwave spectroscopy,[25,26] gas electron diffraction,[27] and photoelectron spectra.[28−30] In particular, these measurements led to contradicting results for the conformational arrangement of the methoxy group in anisole. Electron diffraction[27] and microwave data[25] pointed to planarity of the heavy atom skeleton, while photoelectron spectra[28,29] were interpreted in terms of a mixture of planar and perpendicular conformers. Also Raman spectral data at 130 K suggested the existence of two stable conformers.[31] The present study could shed some light on the structural properties and the rotational barriers of anisole as well as of thioanisole.

The occurrence of the CH symmetric stretching mode for the methyl group of anisole at low wavenumber (~2836 cm^{-1}) still represents a problem under investigation. This evidence could be related to the back-donation process, involving the release of electronic charge of oxygen lone pairs to the σ^* orbitals of the adjacent CH bonds. But Zerbi and co-worker[32] recently excluded this possibility on the basis of HF ab initio calculations, suggesting, instead, a strong Fermi resonance with the first overtone of the symmetric methyl deformation around 1500 cm^{-1}. Thus, a detailed investigation on the CH stretching overtones could also confirm this conclusion.

Experimental Section

Anisole and thioanisole (purity > 99%) from Merck were purified by distillation and then used for both optical absorption spectroscopy and optoacoustic measurements as pure liquids.

The optical absorption spectra were taken with a Cary 5 spectrometer using cuvettes with different path length from 0.1 up to 10 cm in the range 500−2000 nm.

Optoacoustic measurements were performed in the same wavelength range by using as exciting radiation the visible and near-infrared output of an optical parametric oscillator equipped with a β-BBO crystal, pumped by the third harmonic (355 nm) of a nanosecond pulsed Nd:YAG laser with 10 Hz repetition rate. Due to the degeneration of the β-BBO crystal output around 710 nm, it was not possible to explore that range corresponding to the CH stretching fourth harmonic region. The incident beam is vertically focused by means of a $f = 100$ mm cylindrical lens on a 1 cm thick cell. An ultrasonic transducer (Panametrics V103-RM) in contact with the sample cell through a thin grease film detects the pressure wave due to volume expansion of the small absorption region. The method is based on the heat conversion of the nonradiatively relaxed part of the absorbed energy and on the consequent expansion of the absorption volume, which generates an acoustic wave with amplitude P.[20] In the linear absorption regime, P depends on several factors according to the following expression:

$$P \propto \frac{\beta v_a}{C_p} \alpha E_o \qquad (1)$$

where E_o is the laser energy, β the thermal expansion coefficient, C_p the specific heat at constant pressure, v_a the acoustic velocity, and α the linear absorption coefficient of the medium. The spectra were normalized to a reference signal taken by measuring the intensity of the incident beam as a function of wavelength. Both absorption and reference signals were sent to a boxcar for averaging and further processed by a PC for normalization and storing.

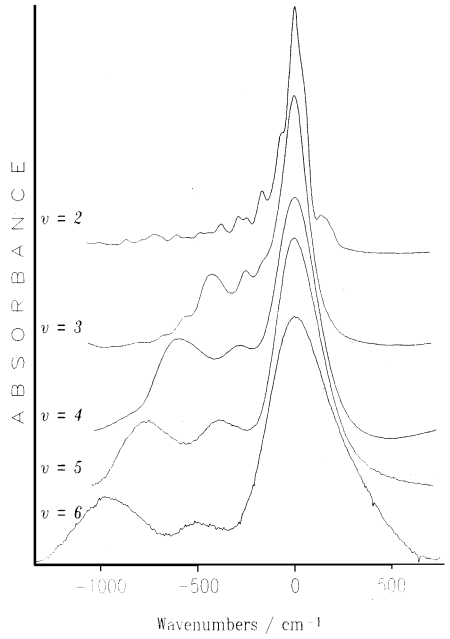

Figure 2. Optical spectra of liquid anisole at room temperature as a function of the vibrational quantum number v.

The Raman spectra have been recorded on liquid anisole by using the 488.0 nm exciting line of an Ar^+ laser, a Jobin-Yvon HG-2S monochromator with 4 cm^{-1} resolution, and a water-cooled RCA-C31034A photomultiplier.

Ab Initio Calculations

DFT ab initio calculations of optimized structures and normal-mode analysis were performed by using the B3-LYP exchange correlation functional and the extended 6-31G(d,p) basis set with the GAUSSIAN 98 suite of programs.[33] The same calculation level was used to determine the energy barrier for both the torsional motions of the methyl group around the $X-C_{met}$ bond and of the $X-C_{met}$ group around the C_1-X bond, where in our case X = O, S. The comparison with calculations on anisole performed at 6-311G++(d,p) level[34] demonstrates the reliability of our results. According to previous DFT calculations,[35] the normal-mode frequencies have been scaled by a factor 0.9613 for the 6-31G(d,p) basis set. For the 6-311G++(d,p) basis set, a satisfactory fit of the experimental data is obtained by scaling the calculated frequencies in the range up to 2000 cm^{-1} by a factor 0.973 and those in the range above 2000 cm^{-1} by a factor 0.963.

Results

The optical spectra of pure anisole and thioanisole are shown in Figure 2 and Figure 3, respectively, as a function of the vibrational quantum number v. The corresponding optoacoustic measurements have identical features and band maxima and, for this reason, are not presented in these figures. The frequencies of the overtone band maxima are listed in Table 1. Three bands are clearly observable up to $v = 6$ in the first case. The most intense band, slightly asymmetric on the high-energy side

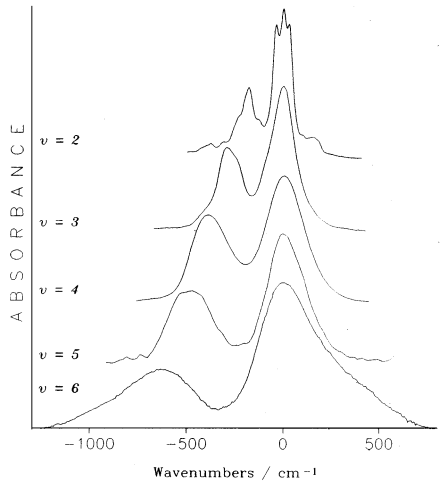

Figure 3. Optical spectra of liquid thioanisole at room temperature as a function of the vibrational quantum number v.

of the spectrum, is easily related to the stretching overtone motion of the C−H ring bonds. The other two bands, whose relative intensity ratio is 1:2, correspond to the nonequivalent methyl C−H stretching overtones. On the other hand, the spectra of thioanisole show only two bands: the most intense is due to aryl C−H stretching overtones, the other to the methyl ones, in this case all equivalent. The same spectral behavior is shown by the optical spectra of toluene, reported for comparison in Figure 4. As the overtone spectra have been measured in the liquid phase, where the peaks are broader than in vapor phase and structural band details can be lost, the reported data should be considered as average values. In fact, the vapor-phase spectra in toluene show highly asymmetric methyl peaks due to effective torsion-stretching coupling,[22] though the methyl torsional barrier is very low. The C−H stretching overtone progressions, depending on the vibrational quantum number v, are satisfactorily fit by a two-parameter equation

$$\nu/v = \varpi - \varpi x\,(v + 1) \tag{2}$$

derived from the energy of the Morse diatomic oscillator, where ϖ and ϖx are, respectively, the mechanical frequency in wavenumber and the anharmonicity.

Only the observed frequencies with local mode characteristics have to be used in eq 2 to obtain the fundamental harmonic frequencies, ϖ, which are related to the corresponding force constants, K, by the equation of the diatomic oscillator localized on the C−H bond

$$2\pi c\varpi = \sqrt{(K/\mu)} \tag{3}$$

where c is the light speed in vacuum and μ the reduced mass.

Previous empirical considerations[2,6,36] let Henry and coworkers[21,37] develop the following equation for a qualitative estimation of the length of C−H bond in angstroms:

$$R_{CH} = 1.084 - (\Delta\nu/11v)\,0.001 \tag{4}$$

where 1.084 is the usual C−H bond length of benzene in angstroms and $\Delta\nu$ the wavenumber shift of the observed overtone with respect to the corresponding overtone of benzene. As reference data, we take the high overtones of benzene detected in the gas phase.[38] In the case of methyl C−H bonds, we consider the C−H bond length of 1.091 Å, typical of aliphatic hydrocarbons, and the high overtones of gaseous ethane.[39]

Together with the spectral maxima, in Table 1 the calculated values of ϖx, ϖ, and K obtained from the experimental data through the relative equations are reported for anisole, thioanisole, and toluene. The DFT optimized structures are shown in Table 2, where for comparison the data from ref 34 are also listed. The vibrational frequencies and their assignment are shown in Table 3.

Discussion

Anisole. The overtone spectral data can be better interpreted if an overview of the fundamental CH stretching region is provided. In fact, the normal mode pattern is complicated by the occurrence of a Fermi resonance and the presence of other bands attributable to overtone or combination modes. In Figure 5, the infrared spectra of anisole in liquid[32] and vapor[40] phases are shown. Some differences can be detected between the two spectra, concerning, in the liquid spectrum, a marked frequency downshift (∼15 cm^{-1}), attributable to intermolecular interactions, and a strong increase of intensity for the symmetric CH_3 stretching mode observed at 2836 cm^{-1}. This latter evidence can be explained by a more efficient Fermi resonance in the liquid, due to a better coincidence with the overtone of the CH_3 deformation mode. Some useful information can be also deduced by the observation of the Raman spectra in polarized light, shown in Figure 6. The band observed at 2838 cm^{-1}, assigned to the symmetric CH_3 stretching, disappears in the spectrum with perpendicular polarization, as well as the bands observed at 2925 and 2945 cm^{-1}, which thus can be considered as overtone modes of the asymmetric and symmetric CH_3 bending deformations, respectively. The depolarized band, observed at 2910 cm^{-1} with weak intensity, is attributable to a combination of the two deformation modes of the methyl group. The band at 2960 cm^{-1}, detected only in the spectrum with perpendicular polarization, is undoubtedly attributable to the asymmetric CH_3 stretching.

The DFT calculation predicts an optimized structure where the methoxy group is lying in the ring plane, together with one hydrogen atom (hereafter called equatorial) of the methyl group (see Table 2 for structural parameters). The two other methyl hydrogen atoms (hereafter called axial) are out of the plane. The ring plane bisects the angle HCH. The DFT-calculated harmonic frequencies are listed in Table 3 together with the proposed assignment, which satisfactorily matches the experimental data.[41]

The equatorial C−H stretching mode observed at 3003 cm^{-1} results not coupled with the motion of other oscillators and also the band detected at 3105 corresponds to a largely uncoupled stretching mode of one aromatic C−H bond. This latter (hereafter called C−H*, see Figure 1) is located in the ortho position with respect to the methoxy substituent, near to the CH_3 group. By considering the double of the frequency calculated at 1464 cm^{-1} (6-311G++(d,p) basis set[34]), an overtone band is predicted for the symmetric deformation of the methyl group near to the symmetric stretching mode calculated at 2891 cm^{-1}. This fact accounts for the occurrence of a Fermi resonance, responsible of the downshift of the C−H stretching band observed in the infrared spectrum at 2836 cm^{-1}, as well as proposed by Zerbi and co-worker.[32] On the other hand, the purely harmonic DFT calculation is able to reproduce the asymmetric C−H stretching mode (obs. 2944 cm^{-1}; calc. 2947 cm^{-1}), but not the symmetric CH_3 stretching vibration observed at low frequency (obs. 2836 cm^{-1}; calc. 2891 cm^{-1}). Hence, a strong anharmonic coupling like that deriving from a Fermi resonance must be effective.

TABLE 1: Observed CH Stretching Overtone Maxima (cm^{-1}) of Anisole, Thioanisole, and Toluene Obtained from Spectrophotometric and Optoacoustic Measurements (anisole and thioanisole only) and their Corresponding Spectral Parameters[a]

	anisole			thioanisole		toluene	
Δv	aryl CH	methyl CH eq/ax[b]		aryl CH	methyl CH	aryl CH	methyl CH
1	3093, 3062, 3032	3003, 2944, 2836		3073, 3060, 3045	3001, 2985, 2918	3087, 3063, 3029	2979, 2952, 2921
2	6103, 5967, 5900	5800, 5719, 5678		5918, 5956, 5984	5777, 5720, 5650	5876, 5908, 5953	5790, 5734, 5649
3	8787	8537	8361	8768	8474	8757	8575
4	11484	11209	10894	11460	11070	11428	10967
5	14055	13665	13285	14020	13540	13986	13439
6	16549	16040	15576	16500	15870	16460	15710
7	18930			18855		18780	
ϖx (cm^{-1})	55.1	63.6	63.5	56.8	61.2	57.6	61.7
ϖ (cm^{-1})	3144	3117	3040	3147	3074	3145	3053
SD (cm^{-1})	1.7	2.1	0.9	1.9	1.2	1.7	3.6
R_{C-H} (Å)	1.084	1.088	1.095	1.085	1.090	1.082	1.090
K (mdyn/Å)	5.415	5.325	5.062	5.428	5.176	5.418	5.106

[a] Δv stands for the vibrational quantum number; ϖx is the anharmonicity constant calculated from eq 2, and ϖ the relative harmonic frequency; SD is the standard deviation value for each linear fit; R_{C-H} indicates the C−H bond length as described in eq 4, and K is the C−H bond force constant (see eq 3). [b] eq = equatorial; ax = axial.

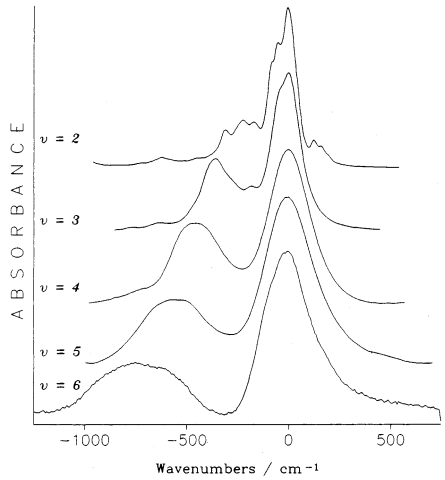

Figure 4. Optical spectra of liquid toluene at room temperature as a function of the vibrational quantum number v.

With this in mind, the analysis of the overtone spectra, shown in Figure 2 up to $\Delta v = 6$ and whose wavenumbers are reported in Table 1, is straightforward. No evidence of Fermi resonance is observed in the first overtone, where the coupling between the C−H oscillators is still present, as found also in the second overtone. For this reason, the observed frequencies with $\Delta v = 2$ and 3 do not correspond to those predicted by the local mode model. From $\Delta v = 4$ to $\Delta v = 7$, instead, the overtones are correctly interpreted in terms of local modes. Thus, by using eq 2, it is possible to evaluate the bond anharmonicities as the slopes of the linear fittings of the ν/v values vs v, as reported in Figure 7, for both optoacoustic and spectrophotometric data. The ϖ and ϖx values of the axial C−H stretching modes are 3040 and 63.5 cm^{-1}, respectively. The equatorial C−H stretching vibration follows quite well the linear fitting with $\varpi = 3117$ cm^{-1} and $\varpi x = 63.6$ cm^{-1}. The anharmonicity of both the methyl C−H stretching vibrations is slightly larger than that observed in toluene (61.7 cm^{-1}) and thioanisole (61.2 cm^{-1}), as shown in Table 1. This means that the nonequivalence should be intrinsic of the methoxy group and not due to steric hindrance with the adjacent hydrogen atom of the ring. A confirmation of this hypothesis comes from SCF MO ab initio calculations on dimethyl ether,[42] which predicted a short length for the CH bond lying in the plane of the heavy atoms. This is in good agreement with the DFT results performed at 6-311G++(d,p)[34] and 6-31G(d,p) level, as shown by the optimized structures reported in Table 2.

TABLE 2: Optimized Structures of Anisole and Thioanisole Obtained from DFT ab Initio Calculation Using the B3-LYP Exchange-Correlation Functional[a]

	anisole		thioanisole
	6-31G(d,p)	6-311G++(d,p)[b]	6-31G(d,p)
C_1-C_2	1.3996	1.3974	1.4002
C_2-C_3	1.3987	1.3976	1.3972
C_3-C_4	1.3923	1.3901	1.3932
C_4-C_5	1.3993	1.3979	1.3975
C_5-C_6	1.3898	1.3878	1.3916
C_6-C_1	1.4029	1.4007	1.4049
C_2-H^*	1.0835	1.0817	1.0838
C_3-H_3	1.0864	1.0845	1.0865
C_4-H_4	1.0854	1.0835	1.0855
C_5-H_5	1.0863	1.0844	1.0863
C_6-H_6	1.0851	1.0834	1.0865
C_1-X	1.3669	1.3660	1.7852
$X-C_{me}$	1.4180	1.4205	1.8215
$C_{me}-H_{eq}$	1.0911	1.0888	1.0918
$C_{me}-H_{ax}$	1.0977	1.0956	1.0924
$C_{me}-H_{ax}$	1.0977	1.0956	1.0924
H^*-H_{ax}	2.3426	2.3496	2.3627
C_2-C_{me}	2.8340	2.8389	3.0682
$H_{ax}-C_{me}-H_{ax}$	108.97	109.42	110.20
C_1-X-C_{me}	118.23	118.61	103.62

[a] Atomic numbering refers to Figure 1. X stands for O or S atom, "me" for methyl, "ax" for axial, and "eq" for equatorial. Bond distances are in Å and bond angles are in degrees. [b] Data from ref 34.

On the basis of the local mode approach, the C−H stretching fundamentals are predicted, accordingly to the expression $\nu = \varpi - 2\,\varpi x$, at 2990 and 2913 cm^{-1} for the equatorial and axial stretching modes, respectively. The first value corresponds to the band observed at 3003 cm^{-1} (Figure 5), which is widely uncoupled, as discussed above on the basis of the DFT results. The second one, due to Fermi resonance, cannot correspond to any experimental values, but results intermediate between the calculated values for the symmetric and asymmetric stretching modes of the methyl group (see Table 3), 2891 and 2947 cm^{-1}, respectively. As Fermi resonance produces a downshift of about 50 cm^{-1} (2891 ⇒ 2836 cm^{-1}) for the methyl C−H stretching fundamental, an analogous upshift is expected for the C−H bending overtone, which should occur at about 2940 cm^{-1}. Just at 2945 cm^{-1} the Raman spectrum (Figure 6) shows a polarized band, attributable to the C−H bending overtone. This finds its

TABLE 3: Calculated and Observed Vibrational Frequencies (cm^{-1}) of Anisole and Thioanisole and Relative Assignment[a]

anisole			thioanisole		
calc.	obs.[41]	calc.[34]	calc.	obs.[45]	assignment
90		88	21		XCH_3 torsion
205	209	198	165		CH_3 torsion
249		249	194	181⊗	C−X−C ip bending
267	263	257	227	230	CH_3 torsion
409	415	409	402	395	CCC twisting
430		434	323	325	CCX ip bending + ip ring deformation
501	511	500	468	478	CCC twisting
539	554	545	407	416	ip CCX, CXC bendings + ip ring deformation
605	617	612	613	613	ip ring deformation
676	690	662	685	688	ring torsion
738	752	736	730		op CCH bendings + ring torsion
771	782	775	678	685	ring−X stretching + ip ring deformation
799	819	802	821	843	op CCH bendings
859	880	859	876	855	op CCH bendings
924		930	940		op CCH bendings
947	975	944	966	984	op CCH bendings
972	992	982	985	1000	triangular ring motion
1009	1019	1013	1025	1024	ring breathing
1039	1039	1036	710	735	$X-CH_3$ stretching
1066	1073	1072	1084	1091	ip CCH bendings
1132		1135	952	969	CH_3 rocking
1138	1151	1146	1156	1148	ip CCH bendings
1154	1172	1162	1182	1186	ip CCH bendings
1165	1180	1169	963	958	CH_3 rocking
1244	1247	1237	1079	1073	ring−X stretching + ip CCH bendings
1294	1292	1298	1293	1275	ip CCH bendings + C═C stretchings
1318	1332	1320	1321	1311	C═C stretchings + ip CCH bendings
1429	1442	1433	1338	1338	CH_3 umbrella motion
1441	1452	1445	1442	(1378)	ring C═C stretchings + ip CCH bendings
1446	1455	1452	1441	1413	HCH asymmetric deformation
1462	1469	1464	1450	1439	HCH symmetric deformation
1486	1497	1485	1484	1480	ring C═C stretchings + ip CCH bendings
1579	1588	1580	1586	1581	ring C═C stretchings
1599	1599	1598	1602	1593*	ring C═C stretchings
2898	2836	2891	2944	2918	methyl C−H symmetric stretchings.
2956	2944	2947	3029	2985	methyl axial C−H asymmetric stretchings
3026	3003	3016	3039	3001	methyl equatorial C−H stretching
3057	3032	3046	3060	3045	ring C−H stretchings
3064		3053	3066	3060	ring C−H stretchings
3081	3062	3069	3076	3073	ring C−H stretchings
3089	3093	3076	3088		ring C−H stretchings
3096	3105	3085	3103		ring C−H* stretching

[a] The first and fourth columns refer to B3-LYP/6-31G(d,p) calculations scaled[35] by a factor 0.9613. The observed data derive from infrared spectra in liquid phase[41,45] (see Figure 5 for the C−H stretching modes of anisole). Thioanisole frequencies labeled as * and ⊗ are taken from refs 45 and 46, respectively. The value in parentheses is assigned as overtone of the 690 cm^{-1} mode. The third column refers to B3-LYP/6-311G++(d,p) values[34] scaled by a factor 0.973 in the range 80−2000 cm^{-1} and by a factor 0.963 above 2000 cm^{-1}. In the assignment, we used the following abbreviation: "ip" = in plane; "op" = out of plane; X = O, S; C−H* = ring C−H bond nearest to the CH_3 group, as shown in Figure 1.

counterpart in the infrared band observed in the liquid at 2944 cm^{-1} (Figure 5).

The force constants of the axial and equatorial localized C−H stretching modes are calculated 5.062 and 5.325 mdyn/Å, respectively. The lengthening of the axial C−H bonds, discussed above, as well as the weakening of the corresponding force constant, can be related to electron back-donation from the lone-pairs of the oxygen atom to the σ^* orbitals of the adjacent C−H bonds.[36] This effect, generally present in methoxy-containing compounds, is mainly relevant when the adjacent hydrogen atoms are in trans conformation with respect to the lone-pairs. In the case of anisole this situation occurs for the axial hydrogen atoms of the methyl group.

In regard to the aryl C−H stretching vibrations, they generally occur in the overtone spectra as a single band (Figure 2), but a shoulder evident at higher wavenumbers is visible for $\Delta v = 6$ and 7, as shown in Figure 8. By deconvolution of these bands the occurrence of two distinct absorption maxima is detected with 4:1 intensity ratio, for the fifth as well as for the sixth overtone. Hence, a shoulder can be identified at about 16855 and 19340 cm^{-1}, respectively. The lengths of the aryl C−H bonds, as obtained by DFT calculations (Table 2), have results practically identical to the corresponding value in benzene (1.084 Å), except for the C−H* bond, in the ortho position with respect to the methoxy group and near to the axial hydrogen atoms, which exhibits a quite short distance, 1.0817 Å (1.0835 Å, with the 6-31G(d,p) basis set). Thus, it is reasonable to consider the weak shoulder as due to the C−H* bond stretching mode, while the other four ring C−H stretching modes behave as nearly equivalent oscillators. The harmonic frequencies, ϖ, are 3135.5 cm^{-1} for the C−H* stretching and 3144 cm^{-1} for the other C−H stretching modes. Actually, the aryl C−H* and C−H bonds have similar force constants (∼5.4 mdyn/Å), but quite different anharmonicities, 46.6 and 55.1 cm^{-1}, respectively. The low anharmonicity of the C−H* stretching can be explained with the H···H interaction with the axial hydrogen atoms of the adjacent methyl group whose distance is shorter (see Table

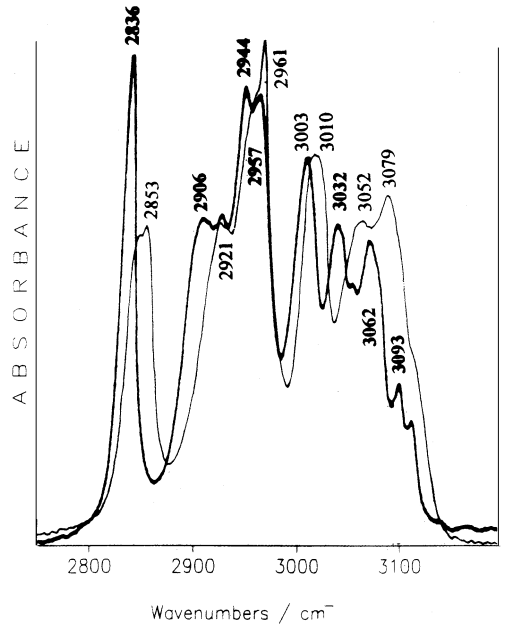

Figure 5. Infrared spectra of anisole in liquid (from ref 32, heavy solid line) and vapor (from ref 40, solid line) phases in the fundamental CH stretching region.

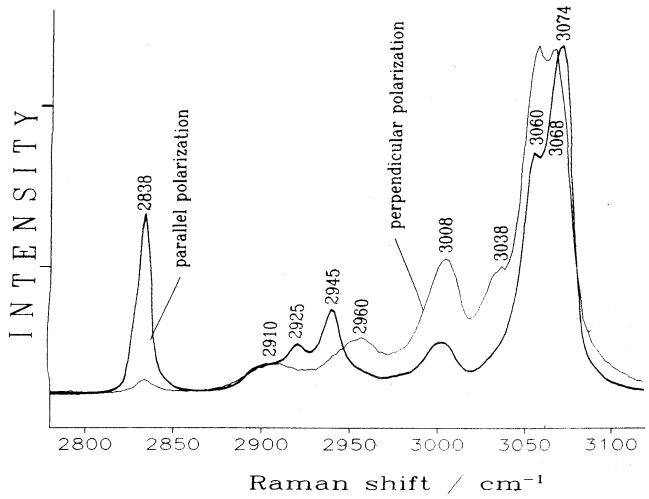

Figure 6. Raman spectra of liquid anisole at room temperature in polarized light in the fundamental CH stretching region ($\lambda_{exc} = 488$ nm). Heavy solid line corresponds to parallel polarization, solid line to perpendicular polarization.

2) than the sum of the van der Waals' radii for hydrogen atoms (2.40 Å).[43]

Finally, it is worthy to note that the fifth overtone of the aryl C−H stretching mode is observed at 16550 cm^{-1}, at a significantly higher frequency with respect to that reported in the literature by Mizugai et al.[4] (16515 cm^{-1}), as obtained by thermal lensing measurements in the liquid phase. On the contrary, we have verified that the fifth overtones of liquid toluene and thioanisole occur at the same frequencies reported by Mizugai et al.[4] To test the overtone wavenumbers in anisole, we have carefully compared the optoacoustic spectrum of this region with the spectrophotometric data, obtaining the same results, as reported in Figure 9. Thus, in anisole the substituent effect on the aromatic system results stronger than previously predicted and quite different with respect to that in toluene and thioanisole.

Thioanisole. The optimized structure of thioanisole, obtained from the DFT calculation, is shown in Table 2, while the

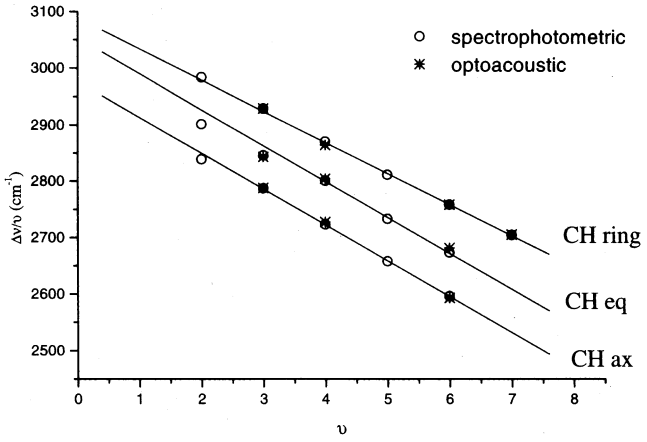

Figure 7. Plot of the function $\Delta\nu/\nu$ as a function of ν, as given in eq 2, for the CH stretching overtone of anisole. The reported data derive respectively from spectrophotometric (○) and optoacoustic (*) spectra. The linear fitting has been done considering only the points with $\Delta\nu \geq 4$, that are correctly interpreted as local modes.

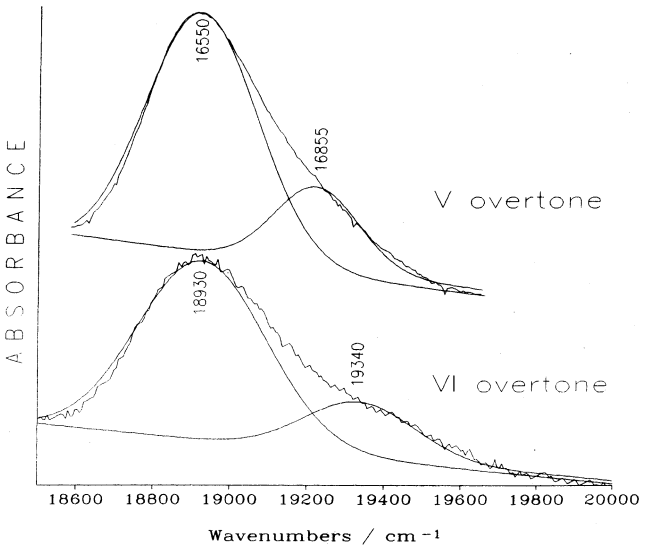

Figure 8. Fifth ($\Delta\nu = 6$) and sixth ($\Delta\nu = 7$) overtones of anisole in the region of the aryl CH stretching vibrations. Superimposed, the deconvolution of these bands is shown.

complete assignment of the vibrational spectrum is reported in Table 3. With respect to previous attribution,[44] some unassigned bands are now considered fundamentals. The infrared band observed at 1378 cm^{-1}, which does not correspond to the calculated mode at 1442 cm^{-1}, is to be considered, instead, as overtone of the very strong band at about 690 cm^{-1}, as actually proposed elsewhere.[45,46] It is evident that the exchange of oxygen with sulfur does not largely affect the ring modes, which are found a few wavenumbers lower in thioanisole than in anisole. Also the H−C−H bending modes of the methyl group in thioanisole undergo small downshifts (~20 cm^{-1}). This accounts for the overtone of the CH_3 symmetric bending mode[44] occurring at about 2850 cm^{-1}, without Fermi resonance with the CH_3 symmetric stretching fundamental, which, instead, occurs at about 2920 cm^{-1}, as predicted by the DFT calculations. The other vibrations involving the X atom of the substituent group are more affected by the presence of sulfur instead of oxygen, mainly those with large contributions of X−CH_3 stretching (1039 ⇒ 735 cm^{-1}) or X−ring stretching (1247 ⇒ 1073 cm^{-1}).

Interesting considerations on the static and dynamic properties of thioanisole can be deduced from the overtone spectra of the C−H stretching vibrations. Only two bands are found for

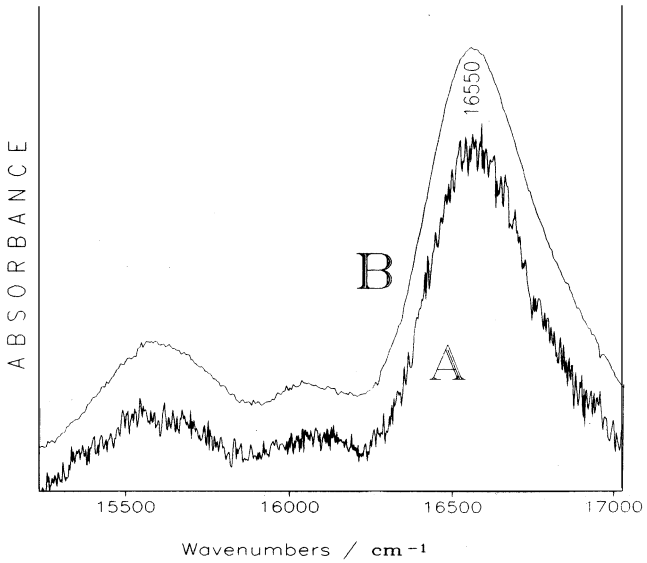

Figure 9. Optical absorption (A) and optoacoustic (B) spectra of liquid anisole at room temperature measured in the region of the fifth overtone.

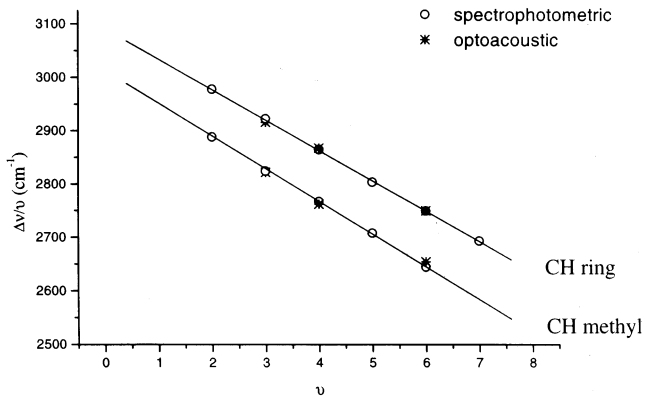

Figure 10. Plot of the function $\Delta\nu/\upsilon$ as a function of υ, as given in eq 2, for the CH stretching overtone of thioanisole. The reported data derive, respectively, from spectrophotometric (○) and optoacoustic (*) spectra. The linear fitting has been done considering only the points with $\Delta\upsilon \geq 4$, that are correctly interpreted as local modes.

thioanisole (see Figure 3), the first related to the aryl CH stretching mode, the second to the methyl CH stretching mode, suggesting that all three bonds of the CH_3 group are equivalent, or in alternative, the rotation is too fast to be revealed through absorption spectroscopy. The anharmonicity constants are evaluated, as well as for anisole, by the linear fittings of the ν/υ values vs υ, as reported in Figure 10 and Table 1, for both optoacoustic and spectrophotometric data. No significant change results in the localized stretching modes of the ring C−H bonds of anisole and thioanisole, which are found near the same wavenumbers in both cases (3144 and 3147 cm^{-1}), and also in toluene (3145 cm^{-1}). The frequency difference observed in the overtone progressions is, instead, due to the difference of anharmonicity constants.

Also in thioanisole the fifth and sixth overtones of the ring C−H stretching modes appear asymmetric, suggesting the presence of a shorter aryl C−H bond, related to a stretching mode at higher wavenumber. Actually, the optimized structure reported in Table 2 exhibits an ortho C−H bond shorter (1.0838 Å) than other ones (∼1.086 Å). This depends, as well as in anisole, on the H···H repulsion with the adjacent hydrogen atoms of the methyl group, owing to a distance (∼2.36 Å) shorter than the sum of the van der Waals' radii.[43] Moreover, this bond corresponds to the highest calculated frequency, 3103 cm^{-1}, practically uncoupled with the motion of the other C−H oscillators.

More significant differences are observed in the overtone spectra of the methyl C−H stretching modes. These latter appear, in the local mode approximation, as equivalent oscillators, as in toluene (Figure 4), with intermediate wavenumbers between those corresponding to axial and equatorial C−H stretching vibrations of anisole. The relative force constant results higher than the corresponding average value of anisole (5.149 mdyn/Å), while the anharmonicity constant is lower. The C−H bond length (1.090 Å), evaluated from the overtone spectra, is the same as in toluene and represents a typical value of aliphatic C−H length. This is in good agreement with the methyl C−H distances calculated by DFT method (∼1.092 Å), as reported in Table 2. The DFT calculations show a planar structure, where the heteroatom and the methyl group lie in the ring plane, as in anisole. On the contrary, the axial and equatorial CH distances are substantially the same, but the CH_3 umbrella is more open with respect to anisole. In thioanisole, the $H_{ax}-C_{me}-H_{ax}$ angle is 110°, while it is 109° in anisole, where it causes less steric hindrance with the ring H* atom. This is not completely surprising when considering the ab initio optimized structures of dimethyl ether[42] and dimethyl sulfide.[47] In these cases, it is interesting to remark that bond angles and distances of the OCH_3 and SCH_3 groups match the corresponding ones in anisole and thioanisole, respectively, as reported in Table 2. This accounts for interpreting the structures and, consequently, the vibrational spectra of the substituent groups on the basis of the intrinsic properties of OCH_3 and SCH_3. In particular, the equivalence of the methyl C−H stretching modes of thioanisole can be considered as depending on the lack of electron back-donation from sulfur to the adjacent methyl C−H bonds, which, instead, occurs in anisole. This effect could be related to a possible free rotation around the S−CH_3 or the S−ring bond.

Rotational Energy Barriers in Anisole and Thioanisole. To better understand the interaction between ring and substituent groups, the rotational barriers of the methyl group around the $C_{me}-X$ (X = O, S) bond and of the XCH_3 groups with respect to the aromatic ring have been evaluated. DFT calculations have been performed at the B3-LYP/6-31G(d,p) level, starting from the optimized geometry of the two molecules, by rotating in steps of 15° or 10°, respectively, the CH_3 or the XCH_3 groups. The structures, finally, have been again optimized, keeping frozen the coordinates of the rotating group. In Figure 11 the results are shown for both molecules, which exhibit a different behavior. The $C_{me}-X$ rotational barrier in anisole is calculated 3.05 Kcal mol^{-1}, and this points to an impaired rotation at room temperature in anisole, whose spectra show nonequivalence between the methyl hydrogen atoms. In thioanisole, instead, the energy barrier is reduced to 1.92 Kcal mol^{-1}, a values that can suggest an easier rotation around the bond. However, the major difference is observed by considering the rotation of the XCH_3 group as a whole, around the bond with the aromatic ring. In this case a strongly hindered rotation is calculated for the methoxy group, being 3.07 Kcal mol^{-1} the energy barrier, accordingly with previous MP2 ab initio calculations.[48] In thioanisole the barrier is only 0.53 Kcal mol^{-1}, indicating the presence of a free rotator in our measuring conditions at room temperature. A justification for such different behavior in the two compounds may be addressed to high electron conjugation of the oxygen atom with the π electrons of the aromatic ring. This effect may cause a stronger stiffness of the methoxy group, keeping it in the planar conformation.

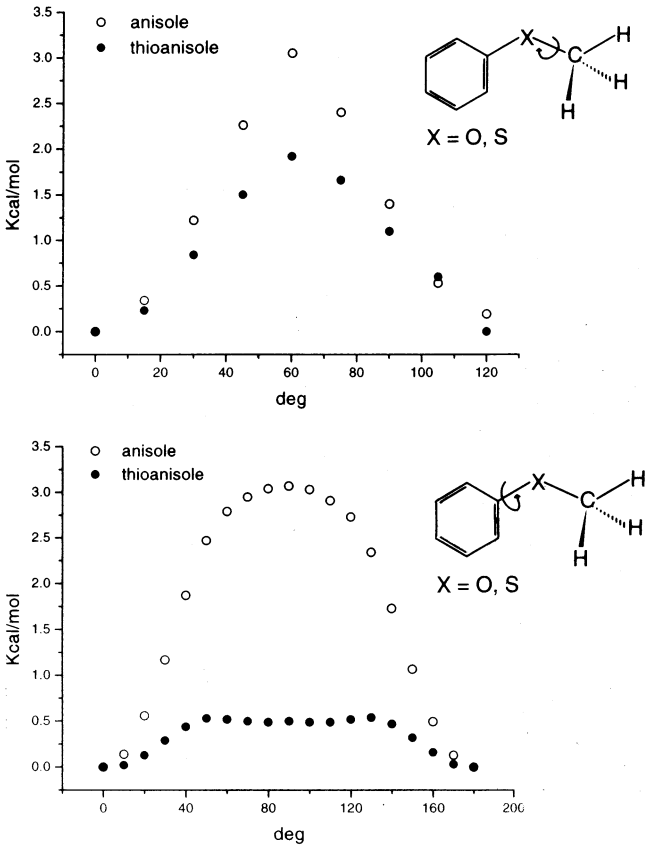

Figure 11. Upper: rotational barrier of the methyl group around the $C_{me}-X$ bond, X = O, S. Lower: rotational barrier of the XCH_3 group with respect to the aromatic ring. Open circle = anisole, full circle = thioanisole. Both calculations have been performed at the B3-LYP/6-31G(d,p) level.

To evaluate the conjugation effect of the heteroatoms toward the aromatic ring, useful information can be obtained from the protonic magnetic resonance.[49] This effect appears relevant in anisole, where the hydrogen atoms in ortho and para positions are more shielded (δ_{ortho}= 6.749; δ_{meta} = 7.145; δ_{para}= 6.811). Otherwise, it is well-known that the methoxy substituent is activating for the electrophilic substitution of the aromatic ring and orienting to the ortho and para positions, where an increase of the negative charge occurs. In thioanisole, instead, the conjugation is quite scarce, as suggested by the similar chemical shifts of the ring hydrogen atoms (δ_{ortho} = 7.158; δ_{meta} = 7.143; δ_{para} = 7.043). The conjugation in anisole affects also the electron charge near the methyl hydrogen atoms, by lowering the back-donation effect with a consequent shielding decrease of these protons with respect to dimethyl ether (δ_{CH_3}(dimethyl ether) = 3.24; δ_{CH_3}(anisole) = 3.757).

Conclusion

In this paper, the high overtones of the CH stretching vibrations of anisole and thioanisole have been investigated by means of optical absorption and optoacoustic measurements. The anharmonic and force constants have been obtained from the experimental data and compared with the corresponding values of toluene. The geometry structures and the vibrational frequencies of anisole and thioanisole have been obtained by DFT ab initio calculations at the B3-LYP/6-31G(d,p) level. A comparison of these results with the experimental data from Raman and IR spectra has allowed a complete assignment of all of the vibrational frequencies of anisole and thioanisole, confirming the presence of a strong Fermi resonance for the methyl C−H symmetric stretching of anisole that occurs at low wavenumber (2836 cm^{-1}).

The same calculation level was used to determine the energy barrier for the torsional motions of both the methyl and the $X-CH_3$ groups. Very different behavior has been observed in anisole with respect to thioanisole, which may be ascribed to a strong electron conjugation of the oxygen atom with the π electrons of the aromatic ring. This interaction may be responsible for the higher rotational barrier of the methoxy group with respect to $S-CH_3$ and, consequently, for the nonequivalence of the methyl C−H bond in anisole, experimentally observed in both the optical absorption and optoacoustic spectra, but not detected in thioanisole.

Acknowledgment. Financial support from the Italian Consiglio Nazionale delle Ricerche (CNR) and Ministero dell'Istruzione, Università e Ricerca (MIUR) is gratefully acknowledged. The authors thank CINECA (Bologna, Italy) for the computer time and are also largely indebted to Prof. Salvatore Califano, who provided unpublished results and useful discussions.

References and Notes

(1) Henry, B. R.; Mohammadi, M. A. *Chem. Phys*. **1981**, *55*, 385.
(2) Wong, J. S.; Moore, C. B. *J. Chem. Phys*. **1982**, *77*, 603.
(3) Henry, B. R.; Mohammadi, M. A.; Thomson, J. A. *J. Chem. Phys*. **1981**, *75*, 3165.
(4) Mizugai, Y.; Katayama, M. *J. Am. Chem. Soc*. **1980**, *102*, 6424.
(5) Katayama, M.; Mizugai, Y. *J. Am. Chem. Soc*. **1981**, *103*, 5061.
(6) Mizugai, Y.; Katayama, M. *Chem. Phys. Lett*. **1980**, *73*, 240.
(7) Sowa, M. G.; Henry, B. R.; Mizugai, Y. *J. Phys. Chem*. **1991**, *95*, 7659.
(8) Sbrana, G.; Muniz-Miranda, M. *J. Phys. Chem*. **1998**, *102*, 7603.
(9) Katayama, M.; Itaya, K.; Nasu, T.; Sakai, J. *J. Phys. Chem*. **1991**, *93*, 10592.
(10) Swofford, R. L.; Long, M. E.; Albrecht, A. C. *J. Chem. Phys*. **1976**, *65*, 179.
(11) Stannard, P. R.; Elert, M. L.; Gelbart, W. M. *J. Chem. Phys*. **1981**, *74*, 6050.
(12) Watson, I. A.; Henry, B. R.; Ross, I. G. *Spectrochim. Acta* **1981**, *37A*, 857.
(13) Halonen, L.; Child, M. S. *Mol. Phys*. **1982**, *46*, 239.
(14) Child, M. S.; Halonen, L. *Adv. Chem. Phys.* **1984**, *57*, 1.
(15) Mills, I. M.; Robiette, A. G. *Mol. Phys*. **1985**, *56*, 743.
(16) Della Valle, R. G. *Mol. Phys.* **1988**, *63*, 611.
(17) Mortensen, O. S.; Henry, B. R.; Mohammadi, M. A. *J. Chem. Phys.* **1981**, *75*, 4800.
(18) Long, M. E.; Swofford, R. L.; Albrecht, A. C. *Science* **1976**, *191*, 183.
(19) Tam, A. C.; Patel, C. K. N. *Appl. Phys. Lett*. **1979**, *34*, 467.
(20) Patel, C. K. N.; Tam, A. C. *Rev. Mod. Phys.* **1981**, *53*, 517.
(21) Gough, K. M.; Henry, B. R. *J. Phys. Chem*. **1984**, *88*, 1298.
(22) Kjaergaard, H. G.; Turnbull, D. M.; Henry, B. R. *J. Phys. Chem. A* **1997**, *101*, 2589.
(23) Kjaergaard, H. G.; Turnbull, D. M.; Henry, B. R. *J. Phys. Chem. A* **1998**, *102*, 6095.
(24) Kjaergaard, H. G.; Rong, Z.; McAlees, A. J.; Howard, D. L.; Henry, B. R. *J. Phys. Chem. A* **2000**, *104*, 6398.
(25) Onda, M.; Toda, A.; Mori, S.; Yamaguchi, I. *J. Mol. Struct*. **1986**, *144*, 47.
(26) Velino, B.; Melandri, S.; Caminati, W.; Favero, P. G. *Gazz. Chim. Ital*. **1995**, *125*, 373.
(27) Seip, H. M.; Seip, R. *Acta Chem. Scand.* **1993**, *27*, 4024.
(28) Friege, H.; Klessinger, M. *Chem. Ber.* **1979**, *112*, 1614.
(29) Dal Colle, M.; Distefano, G.; Jones, D.; Modelli, A. *J. Phys. Chem. A* **2000**, *104*, 8227.
(30) Eisenhardt, C. G.; Gemechu, A. S.; Baumgartel, H.; Chelli, R.; Cardini, G.; Califano, S. *Phys. Chem. Chem. Phys.* **2001**, *3*, 5358.
(31) Konschin, H.; Tylli, H.; Grundfelt-Forsius, C. *J. Mol. Struct.* **1981**, *77*, 51.
(32) Rumi, M.; Zerbi, G. *J. Mol. Struct.* **1999**, *509*, 11.
(33) Frisch, M. J.; Trucks, G. W.; Schlegel, H. B.; Scuseria, G. E.; Gill, P. M. W.; Stratmann, R. E.; Burant, J. C.; Dapprich, S.; Millam, J. M.; Daniels, A. D.; Kudin, K. N.; Strain, M. C.; Farkas, O.; Tomasi, J.; Barone, V.; Cossi, M.; Cammi, R.; Mennucci, B.; Pomelli, C.; Adamo, C.; Clifford, S.; Ochterski, J.; Johnson, B. G.; Robb, M. A.; Cheeseman, J. R.; Keith, T.; Petersson, G. A.; Montgomery, J. A.; Raghavachari, K.; Al-Laham, M.

A.; Zakrzewski, V. G.; Ortiz, J. V.; Foresman, J. B.; Cioslowski, J.; Stefanov, B. B.; Liu, G.; Liashenko, A.; Piskorz, P.; Komaromi, I.; Cui, Q.; Morokuma, K.; Nanayakkara, A.; Challacombe, M.; Malik, D. K.; Rabuk, A. D.; Peng, C. Y.; Ayala, P. Y.; Chen, W.; Wong, M. W.; Andres, J. L.; Replogle, E. S.; Gomperts, R.; Martin, R. L.; Fox, D. J.; Binkley, J. S.; Defrees, D. J.; Baker, J.; Stewart, J. P.; Head-Gordon, M.; Gonzalez, C.; Pople, J. A. *Gaussian 98, Revision A.9*; Gaussian, Inc.; Pittsburgh, PA, 1998.

(34) Califano, S., private communication.

(35) Scott, A. P.; Radom, L. *J. Phys. Chem.* **1996**, *100*, 16502.

(36) McKean, D. C. *Chem. Soc. Rev.* **1978**, *7*, 399.

(37) Gough, K. M.; Henry, B. R. *J. Am. Chem. Soc.* **1984**, *106*, 2781.

(38) Reddy, K. V.; Heller, D. F.; Berry, M. J. *J. Chem. Phys.* **1982**, *76*, 2814.

(39) Crofton, M. W.; Stevens, C. G.; Klenerman, D.; Gutow, J. H.; Zare, R. N. *J. Chem. Phys.* **1988**, *89*, 7100.

(40) *EPA vapor phase FTIR Library*; ThermoGalactic; Salem, USA, 2001.

(41) Balfour, W. J. *Spectrochim. Acta A* **1983**, *39*, 795.

(42) McKean, D. C.; Kindness, A.; Wilkie, N.; Murphy, W. F. *Spectrochim. Acta A* **1996**, *52*, 445.

(43) *Handbook of Chemistry and Physics*, 60th ed.; Weast, R. C., Ed.; CRC Press Inc.: Boca Raton, FL, 1980.

(44) Cataliotti, R. S.; Paliani, G.; Santini, S. *J. Raman Spectrosc.* **1988**, *19*, 161.

(45) Balfour, W. J.; Chandrasekhar, K. S.; Kyca, S. P. *Spectrochim. Acta A* **1986**, *42*, 39.

(46) Green, J. H. S. *Spectrochim. Acta* **1962**, *18*, 39.

(47) Tsuboyama, A.; Takeshita, K.; Konaka, S.; Kimura, M. *Bull. Chem. Soc. Jpn.* **1984**, *57*, 3589.

(48) Tsuzuki, S.; Houjou, H.; Nagawa, Y.; Hiratani, K. *J. Phys. Chem. A* **2000**, *104*, 1332.

(49) Llabres, G.; Baiwir, M.; Christiaens, L.; Denoel, J.; Laitem, L.; Piette, J. *Can. J. Chem.* **1978**, *56*, 2008.